

Difference Equations for Two-Dimensional Elastic Flow¹

A. G. PETSCHKE² AND M. E. HANSON

New Mexico Institute of Mining and Technology, Socorro, New Mexico 87801

Received June 26, 1968

ABSTRACT

An improved technique for handling two-dimensional elastic flow is applied to several physical problems. The method differs from older methods in that no unresisted distortions of the mesh are allowed. A much quieter mesh results, and more information can be extracted from the calculation.

I. INTRODUCTION

The standard method for handling two-dimensional elastic-plastic flow has been published by Wilkins [1]. In this method the strain rates in a mesh are computed from the velocities and coordinates of the grid intersections in such a way that only the difference in the velocity or coordinate of points diagonally opposite one another on the mesh appear. That is, for instance,

$$\dot{\epsilon}_{xx} = (2A)^{-1}[(\dot{x}_2 - \dot{x}_4)(y_3 - y_1) - (\dot{x}_3 - \dot{x}_1)(y_2 - y_4)] \quad (1)$$

Here A is the area of the mesh, the dot indicates differentiation with respect to time and the grid intersections have been numbered counterclockwise around the mesh, so that \dot{x}_2 indicates the x velocity of the second point. Because the relative displacement of adjacent points does not appear in (1), all the strains, and hence stresses, are computed to be zero unless the diagonals of the mesh are distorted. Consequently, if one visualizes the grid intersections labeled as in an alkali-halide plane, the calculation resists only weakly distortions in which the alkali sublattice moves as a whole with respect to the halide sublattice. This allows unphysical distortions to appear which must be damped out by use of various artificial viscosities.

¹ This work was supported by the Advanced Research Projects Agency and was monitored by the Air Force Office of Scientific Research under Contract F44620-67-C-0113.

² Present address: Systems Science and Software, Inc. Box 1620, La Jolla, California.

That there must be distortions which do not lead to restoring forces can also be seen as follows: in two dimensions there are only four linear components of strain. On the other hand complete specification of the rotation and distortion of a quadrilateral requires six parameters. There must therefore be a two-dimensional manifold of distortions that leads to the same calculated stresses.

While calculating the dynamic distortions of a beam, and in similar problems solved preparatory to a study of fracture phenomena in rock, we noticed the unphysical distortions which result using the technique just described, and it occurred to us to remedy the situation by representing the rigidity of the mesh more or less correctly. The following section describes such a method and the last section describes some applications.

II. THE METHOD

Evidently, one ought to difference the equations so that there are no unresisted distortions of the mesh. We have chosen to do that as follows: consider a quadrilateral which was originally rectangular and had its lower left hand corner at X, Y . Let the lower left hand corner now be displaced to x, y and the point originally at $X + U, Y + V$ be displaced to $x + u, y + v$. Expand the present position as a function of the original position as follows

$$\begin{aligned} u &= aU + bV + cUV + \dots \\ v &= dU + eV + fUV + \dots \end{aligned} \quad (2)$$

We have written down just six parameters in the expansion because this is enough to specify completely the positions of the corners and is as many as can be determined by those positions. The term proportional to UV is preferable to one proportional to U^2 or V^2 because it maps the edges of the original rectangle into straight lines and this ensures that the meshes of the distorted lattice fit together without gaps or overlap.

The coefficients a through f may be found from the coordinates of the grid. That is, if the intersections of grid lines around the mesh are numbered from 1 to 4 as before, the one with $U = V = 0$ is numbered 1, and the original rectangle had the dimensions L by K , then a through f are found from

$$\begin{aligned} u_2 &= aL, & v_2 &= dL, \\ u_3 &= aL + bK + cKL, & v_3 &= dL + eK + fKL, \\ u_4 &= bK, & v_4 &= eK. \end{aligned} \quad (3)$$

Given a through f , one may compute the displacements $u - U$ and $v - V$ and from the displacements the strains as a function of position throughout the mesh.

To compute accelerations, we bisect each mesh in the X and Y directions, associate the masses of the four adjacent quarter zones with each mesh point and compute the force by integrating the stress around the circumference of the mass. To do this the stresses on the line segments $U = L/2$, $0 < V < K/2$; $U = L/2$, $K/2 < V < K$ and so forth are required. These can easily be computed from the strains, provided proper account is taken of the rotation of the mesh. To do the latter, we rotated the zone until the line along which the stress was to be computed, i.e. $V = K/2$ or $U = L/2$ was parallel to its original direction, i.e. the X or Y axis. This implies a rotation through an angle

$$\theta = \tan^{-1} \frac{d + fK/2}{a + cK/2} \quad (4)$$

in the former case and an angle

$$\phi = \tan^{-1} \frac{b + cL/2}{e + fL/2} \quad (5)$$

in the latter. If the rotations are not taken into account, Hooke's law as used below will give rise to large fictitious stresses.

After rotation the strain in the x direction along the line of constant V is

$$\epsilon_{x'}^{\theta} = (a + \frac{1}{2}cK) \cos \theta + (d + \frac{1}{2}fK) \sin \theta - 1. \quad (6)$$

The primes indicate that a rotated coordinate system is in use.

The stresses are, in the case of plane strain (no distortion perpendicular to the plane considered) by Hooke's law, for instance

$$\begin{aligned} \sigma_{y'y'} &= (2\mu + \lambda)[(e + fU) \cos \theta - (b + cU) \sin \theta - 1] \\ &+ \lambda[(a + \frac{1}{2}cK) \cos \theta + (d + \frac{1}{2}fK) \sin \theta - 1]. \end{aligned} \quad (7)$$

Where λ and μ are Lamé constants and the first subscript designates the normal to the surface across which a stress in the direction of the second subscript is exerted.

The corresponding forces are obtained by integrating along the appropriate half bisector of the mesh to give, for instance

$$\begin{aligned} F_{y'y'} &= \int dU \sigma_{y'y'} = (2\mu + \lambda)[(e + \frac{1}{4}f\alpha L) \cos \theta - (b + \frac{1}{4}c\alpha L) \sin \theta - 1] \frac{1}{2}L \\ &+ \lambda[(a + \frac{1}{2}cK) \cos \theta + (d + \frac{1}{2}fK) \sin \theta - 1] \frac{1}{2}L, \end{aligned} \quad (8)$$

where the limits on the integral are 0 and $L/2$ or $L/2$ and L , and α is 1 in the former

case and 3 in the latter. Then the force is rotated back into the original Eulerian frame, that is

$$\begin{aligned} F_{y'y} &= F_{y'y'} \cos \theta + F_{y'x'} \sin \theta, \\ F_{y'x} &= -F_{y'y'} \sin \theta + F_{y'x'} \cos \theta. \end{aligned} \quad (9)$$

Finally the force is summed over the eight line segments surrounding the intersection, and is used to accelerate the mass centered there. A full set of difference equations appears in the Appendix.

Physically, the procedure just described appears reasonable. Others have applied similar, and more elaborate, techniques to problems in statics ([2], [3]). In those calculations, a square is deformed into a quadrangle, and the forces required at the corners are computed, for the case of plane stress and Poisson ratio $1/3$. Given a displacement in the x direction at point 3, Pian [3] finds, in an approximation like ours

$$\begin{aligned} f_{x1} &= -0.2500, f_{x2} = 0.0625, f_{x3} = 0.5000, f_{x4} = 0.3125, f_{y1} = -0.1875, \\ f_{y2} &= 0, f_{y3} = 0.1875, f_{y4} = 0. \end{aligned} \quad (10)$$

Here, f_{x1} is the force in the x direction at point 1 divided by the product of Young's modulus, the plate thickness and the displacement of point 3. In his best approximation he finds [4]

$$\begin{aligned} f_{x1} &= -0.27771, f_{x2} = 0.09021, f_{x3} = 0.47229, f_{x4} = -0.28479, \\ f_{y1} &= 0.1875, f_{y2} = 0, f_{y3} = 0.1875, f_{y4} = 0, \end{aligned} \quad (11)$$

so that convergence appears quite good. Our technique, however, does not compute the force on a corner, but rather the force on a quarter of the zone. Modified to the plane stress case, it leads to forces somewhat different from Pian's, namely

$$\begin{aligned} f_{x1} &= -0.1875, f_{x2} = 0, f_{x3} = 0.5625, f_{x4} = -0.3750, f_{y1} = -0.1875, \\ f_{y2} &= 0, f_{y3} = 0.1875, f_{y4} = 0. \end{aligned} \quad (12)$$

For static problems with short wavelength disturbances, then, our code will probably not give the best possible answer. One could of course write the code so as to use Pian's coefficients, but it is hard to say which set will give the best answers in a dynamic problem.

Since $f_{x2} + f_{x3}$ is the same in all the cases, a simple plane compression wave will have the same speed regardless of which formulation is chosen. Likewise $f_{x1} + f_{x2}$, which determines the shear wave speed, is alike in both approximations. Indeed,

any reasonable approximation must give the same answers for the pure linear compression case and pure shear case, and give zero for the total force in any static distortion, so that there is really only one free parameter. Inasmuch as we believe the essential point to be that the lattice resists all possible distortions, we have made no effort to optimize the free parameter.

III. EXAMPLES

We have examined a beam 10.5 cm long, 1 cm high and infinitely wide simply supported $\frac{1}{4}$ cm from the ends and subjected to a displacement at the center. The steel was taken to have density 7.84 gm/cm^3 and Lamé constants $\lambda = 1.185$, $\mu = 0.79$ megabars. The dilatational sound speed in this material is $0.594 \text{ cm}/\mu \text{ sec}$ and the elastic constant appropriate for use in the thin plate approximation (no stress in one direction and no strain in a perpendicular direction) is 2.2571 which gives a period for the fundamental flexural mode of $450 \mu \text{ sec}$, ignoring the fact that the constraint is not exactly at the end. The point at the top of the center of the beam was moved downward at a speed of $0.001 \text{ cm}/\mu \text{ sec}$ for $50 \mu \text{ sec}$ and then held still. Figure 1 gives some results of the calculation. Figure 1a is a plot of the mesh as calculated by the TEMS code, which relies on the technique just described, at a time of $150 \mu \text{ sec}$. In order to make the distortion visible, it has been amplified by a factor 10, that is 10 times the present coordinate of the point minus 9 times the original coordinate has been plotted. It can be seen that higher modes of the beam are excited and indeed plots made at earlier times show a ringing with a period of about $100 \mu \text{ sec}$ as expected for the first harmonic. For comparison Figure 1b is a similarly amplified plot of the result of applying the POP code which is derived from Wilkins' HEMP code to the same problem, and Figure 1c is an unamplified plot of the same result. A tensor viscosity and a small Richtmyer-von Neumann viscosity were used in the latter calculation. No viscosity was used in the former.

As another example, a beam of the same material, 0.16 cm high and 4 cm long, simply supported at the ends, was subjected to a moving load. A force of 10^{-3} megabars per centimeter was spread out over half a zone (0.02 cm) and moved with a velocity of $0.1 \text{ cm}/\mu \text{ sec}$. This problem, with a point load and in the usual approximation that the rotational inertia of the beam cross section may be ignored, has a well known analytic solution ([5], [6]). Because of the dispersion of flexural wave speeds, a train of waves moving with about twice the load speed moves ahead of the load, and leads to both upward and downward displacements. This is probably clearer from the form of Steele's solution [6] than from the classical finite beam Fourier series solution [5]. Figure 2 exhibits the formation of the wave train, as computed by TEMS. In each case, the line above represents the appropriate analytic solution.

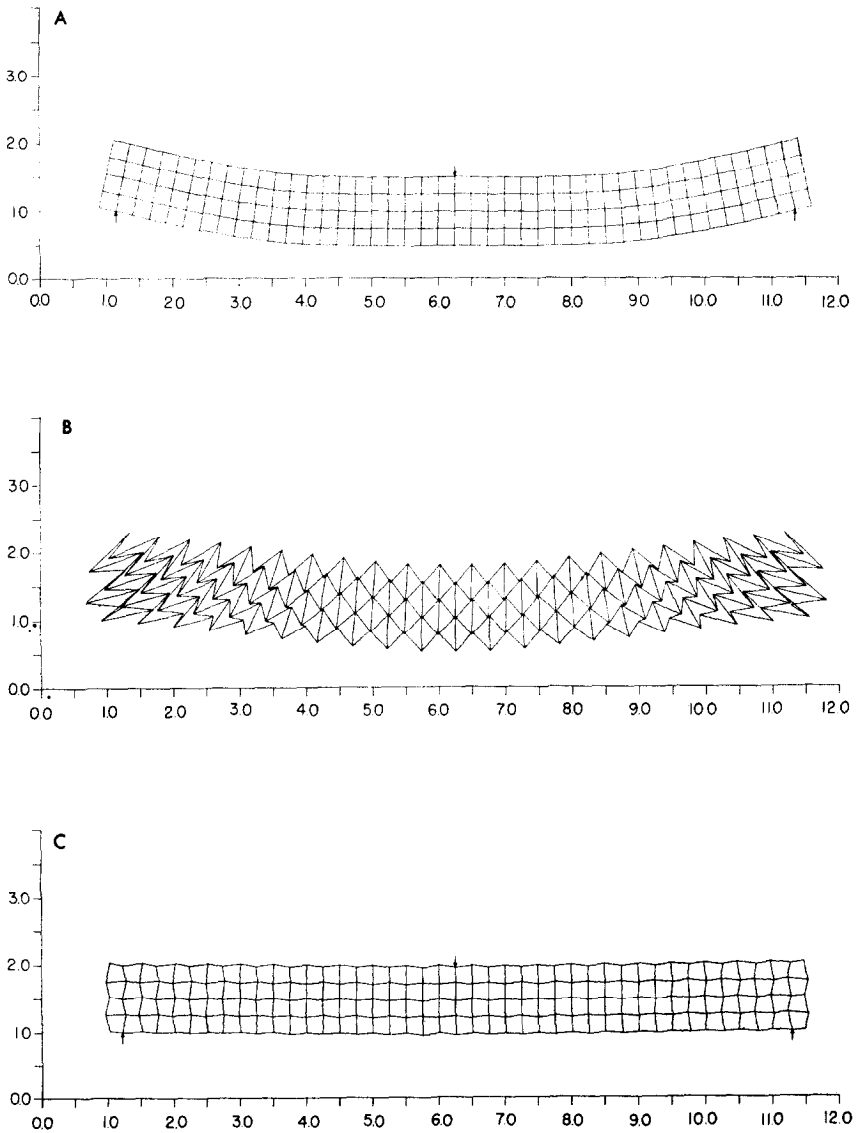


FIG. 1. The deflection of a beam subjected to a displacement at its center, see text for precise description. In part a of the figure, the mesh is given by the calculation described in the text. To make the displacements visible, they have been exaggerated by a factor of 10. In part b, the mesh is given by a HEMP-like calculation with the displacements similarly exaggerated. The relative motion of alternate mesh points is clearly evident. Part c, same as b without exaggeration.

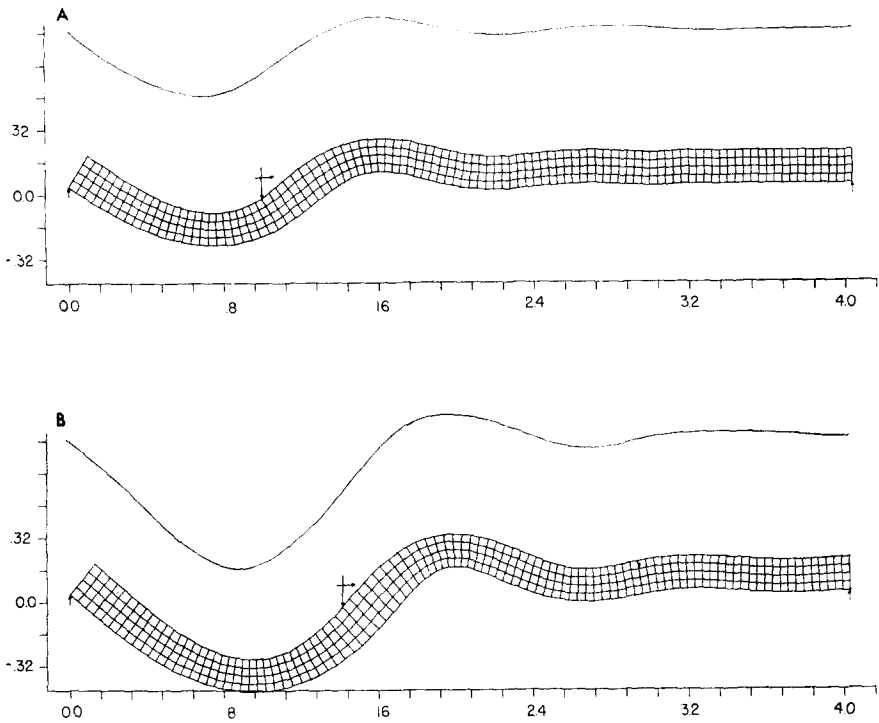


FIG. 2. The deflection, exaggerated by a factor of 10, of a beam subject to a moving load. The line above the beam gives the theoretical deflection for a thin beam. The arrow indicates the position of the load. The formation of a wave train moving ahead of the load is clearly evident. Part a at 10 μ sec; b at 14 μ sec.

IV. CONCLUSION

The method that has been described, when applied to some elementary problems significantly reduces the noise in the mesh observed with previous methods. The application of this method to various problems in seismology and fracture is being carried out by one of us, and will be published elsewhere.

ACKNOWLEDGMENTS

The Steele and Timoshenko-Young solutions for the moving load were coded for us by Mr. Byron Eppler, who also assisted in other ways. Mr. Richard Thorp assisted in operating the computer and developing computer plot routines.

APPENDIX. FINITE DIFFERENCE EQUATIONS FOR THE TWO DIMENSIONAL ELASTIC DYNAMICS CODE "TEMS"

This description is given in rectangular coordinates.

A. THE CALCULATIONAL GRID AND MASS ZONING

A two dimensional Lagrangian grid is placed in the material dividing the material into rectangles. Figure 3 is a schematic of the grid and a numbering system for the center and corners of the zones used in this description of the code. In particular

$$\begin{aligned}
 \textcircled{1} &= k + \frac{1}{2}, l + \frac{1}{2} & 1 &= k, l \\
 \textcircled{2} &= k + \frac{1}{2}, l - \frac{1}{2} & 2 &= k, l + 1 \\
 \textcircled{3} &= k - \frac{1}{2}, l - \frac{1}{2} & 3 &= k + 1, l + 1 \\
 \textcircled{4} &= k - \frac{1}{2}, l + \frac{1}{2} & 4 &= k + 1, l
 \end{aligned}$$

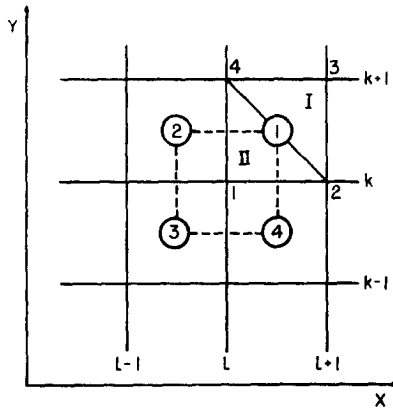


FIG. 3. The grid and numbering scheme for the difference equations.

The mass at each vertex of the rectangles is calculated initially (at time zero) and held constant for the entire calculation. This ensures conservation of mass in the calculation. The mass concentrated at each vertex is taken as $\frac{1}{4}$ the sum of the masses of the adjoining zones. For example:

$$\begin{aligned}
 m_{\textcircled{1}} &= \rho_{\textcircled{1}}^0 A_{\textcircled{1}}^0, \\
 m_{k,l} &= \frac{1}{4}(m_{\textcircled{1}} + m_{\textcircled{2}} + m_{\textcircled{3}} + m_{\textcircled{4}}).
 \end{aligned}
 \tag{A1}$$

The masses at the other vertices are calculated similarly. The area of a quadrangle is taken as

$$\begin{aligned} A_{\Phi}^n &= (A_I)_{\Phi}^n + (A_{II})_{\Phi}^n, \\ (A_I)_{\Phi}^n &= \frac{1}{2}[x_2^n(y_3^n - y_4^n) + x_3^n(y_4^n - y_2^n) + x_4^n(y_2^n - y_3^n)], \\ (A_{II})_{\Phi}^n &= \frac{1}{2}[x_2^n(y_4^n - y_1^n) + x_4^n(y_1^n - y_2^n) + x_1^n(y_2^n - y_4^n)]. \end{aligned} \quad (A2)$$

A_I and A_{II} are the areas of the triangles I and II .

B. STATE EQUATIONS

The compression at cycle n is given by

$$\eta_i^n = \left[\frac{\rho^n}{\rho^0} \right]_i = \left[\frac{A^0}{A^n} \right]_i \quad (A3)$$

The code permits the effective bulk modulus to be given by an expansion of the form

$$K_i^n = \left[\frac{\partial \rho}{\partial \eta} \right]_i^n = a + 2b(\eta_i^n - 1) + 3c(\eta_i^n - 1)^2 + 4d(\eta_i^n - 1)^3, \quad (A4)$$

where the coefficients $b, c, d \dots$ are empirical fits to experimental shock data and can be found in the literature, for example Walsh et al. [7]. The coefficient a is the linear bulk modulus of the material. Given one of the Lamé constants and Poisson's ratio the remaining Lamé constants can be found for linear elasticity. Poisson's ratio is taken to be constant so that the Lamé "constants" are given by

$$\mu_i^n = \frac{3}{2} K_i^n \left(\frac{1 - 2\nu}{1 + \nu} \right), \quad \lambda_i^n = \frac{2\mu_i^n \nu}{1 - 2\nu}, \quad (A5)$$

where μ is the shear modulus and ν is Poisson's ratio.

C. STRAINS AND STRESSES

Consider a rectangle whose original corners were at (X, Y) , $(X + L, Y)$, $(X + L, Y + K)$, $(X, Y + K)$ and let the corners presently be at (x, y) , $(x + l_2, y + k_2)$, $(x + l_3, y + k_3)$, $(x + l_4, y + k_4)$ as shown on Figure 4.

Now consider a point whose original coordinate was $(X + U, Y + V)$ and whose present coordinate is $(x + u, y + v)$. Expand u and v as in Eq. (2).

The coefficients a through f can be obtained by solving Eq. (3) which gives

$$\begin{aligned} a^n &= l_2/L, & b^n &= l_4/K, & d^n &= k_2/L, & e^n &= k_4/K, \\ c^n &= (l_3 - l_2 - l_4)/LK & f^n &= (k_3 - k_2 - k_4)/LK \end{aligned} \quad (A6)$$

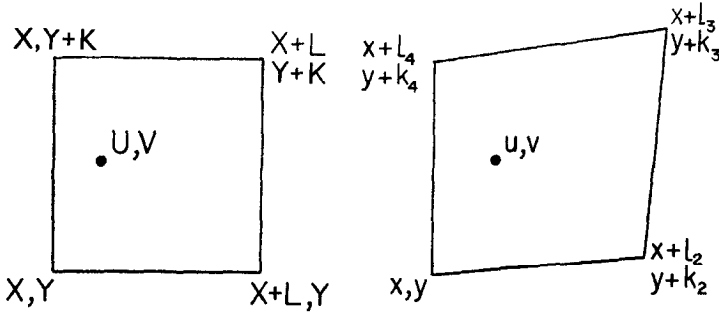


FIG. 4. Comparison of undistorted and distorted meshes indicating the meaning of u and v .

The distortion of the grid will produce, in general, both a rotation and a distortion of each individual mesh. As the rotation will lead to strains which, by Hooke's law, Eq. (A10), produce large stresses, it is necessary to account for the rotations separately. In the distorted mesh, a line of constant V has a slope given by Eq. (4). Rotating the distorted mesh through the angle $-\theta$ puts this line parallel to its original orientation. After rotation through this angle, the point originally at U, V is at u', v' where

$$\begin{aligned} u' &= u \cos \theta + v \sin \theta, \\ v' &= v \cos \theta - u \sin \theta. \end{aligned} \tag{A7}$$

The strains are accordingly

$$\begin{aligned} (\epsilon_x^\theta)^n &= \frac{\partial(u' - U)^n}{\partial U} = (a + cV)^n \cos \theta^n + (d + fV)^n \sin \theta^n - 1, \\ (\epsilon_y^\theta)^n &= \frac{\partial(v' - V)^n}{\partial V} = (e + fU)^n \cos \theta^n - (b + cU)^n \sin \theta^n - 1, \\ (\gamma_{y'x'}^\theta)^n &= \frac{\partial(v' - V)^n}{\partial U} + \frac{\partial(u' - U)^n}{\partial V} = (b + cU)^n \cos \theta^n + (e + fU)^n \sin \theta^n. \end{aligned} \tag{A8}$$

Eliminating the trigonometric functions by use of Eq. (4) gives

$$\begin{aligned} (\epsilon_x^\theta)^n &= (\sqrt{(a + cV)^2 + (d + fV)^2} - 1)^n, \\ (\epsilon_y^\theta)^n &= \left[\frac{(ae - bd) + U(af - dc) + V(ec - bf)}{\sqrt{(a + cV)^2 + (d + fV)^2}} - 1 \right]^n, \\ (\gamma_{y'x'}^\theta)^n &= \left[\frac{(b + cU)(a + cV) + (d + fV)(e + fU)}{\sqrt{(a + cV)^2 + (d + fV)^2}} \right]^n; \end{aligned} \tag{A9}$$

using Hooke's Law, the stresses at a point along the line of constant V are

$$\begin{aligned}(\sigma_{v'v'})^n &= (2\mu + \lambda)^n (\epsilon_{v'}^\phi)^n + \lambda^n (\epsilon_{x'}^\phi)^n \\(\sigma_{v'x'})^n &= \mu^n (\gamma_{v'x'}^\phi)^n.\end{aligned}\tag{A10}$$

Similarly a line of constant U in the distorted mesh has a slope given by Eq. (5). Rotating the distorted mesh through the angle $-\phi$ puts this line parallel to its original orientation. After rotation the point originally at U, V is at u', v' where

$$\begin{aligned}u' &= u \cos \phi - v \sin \phi,^3 \\v' &= v \cos \phi + u \sin \phi;\end{aligned}\tag{A11}$$

the strains are accordingly

$$\begin{aligned}(\epsilon_{x'}^\phi)^n &= \frac{\partial(u' - U)^n}{\partial U} = (a + cV)^n \cos \phi^n - (d + fV)^n \sin \phi^n - 1, \\(\epsilon_{v'}^\phi)^n &= \frac{\partial(v' - V)^n}{\partial V} = (e + fU)^n \cos \phi^n + (b + cU)^n \sin \phi^n - 1, \\(\gamma_{x'v'}^\phi)^n &= \frac{\partial(v' - V)^n}{\partial U} + \frac{\partial(u' - U)^n}{\partial V} = (d + fV)^n \cos \phi \\&\quad + (a + cV)^n \sin \phi^n.\end{aligned}\tag{A12}$$

Again eliminating the trigonometric functions with Eq. (5) gives

$$\begin{aligned}(\epsilon_{x'}^\phi)^n &= \left[\frac{(ae - b d) + U(af - dc) + V(ec - bf)}{\sqrt{(e + fU)^2 + (b + cU)^2}} - 1 \right]^n \\(\epsilon_{v'}^\phi)^n &= (\sqrt{(e + fU)^2 + (b + cU)^2} - 1)^n, \\(\gamma_{x'v'}^\phi)^n &= \left[\frac{(a + cV)(b + cU) + (d + fV)(e + fU)}{\sqrt{(e + fU)^2 + (b + cU)^2}} \right]^n,\end{aligned}\tag{A13}$$

the stresses at a point along the line $U = \text{constant}$ are

$$\begin{aligned}(\sigma_{x'x'})^n &= (2\mu + \lambda)^n (\epsilon_{x'}^\phi)^n + \lambda^n (\epsilon_{v'}^\phi)^n, \\(\sigma_{x'v'})^n &= \mu^n (\gamma_{x'v'}^\phi)^n.\end{aligned}\tag{A14}$$

³ The angle ϕ is taken positive in the clockwise direction and the angle θ is taken positive in the counterclockwise direction.

Occasionally it has been desirable to recover the stress field in the original frame in which case the stresses in the interior of the zone are defined by

$$\begin{aligned}(\sigma_{xx})^n &= (\sigma_{x'x'})^n \cos^2 \psi + (\sigma_{y'y'})^n \sin^2 \psi - 2(\tau_{x'y'})^n \sin \psi \cos \psi, \\(\sigma_{yy})^n &= (\sigma_{y'y'})^n \cos^2 \psi + (\sigma_{x'x'})^n \sin^2 \psi + 2(\tau_{x'y'})^n \sin \psi \cos \psi,\end{aligned}\tag{A15}$$

where

$$\begin{aligned}\tau_{x'y'} &= (\sigma_{y'x'} + \sigma_{x'y'})^n/2, \\ \tan \psi &= (\tan \theta^n - \tan \phi^n)/2.\end{aligned}\tag{A16}$$

This amounts to averaging the rotation and shear stresses computed along the lines $U = \text{constant}$ and $V = \text{constant}$.

D. THE MOMENTUM EQUATIONS

For the dynamics, the stresses are integrated on the quarter zones about the mass point k, l . For example, the integration is carried out along the dashed line segments about the mass point k, l in Figure 3.

We must integrate the appropriate stresses along the line $V = K/2$ over the segment $0 \leq U \leq L/2$ or $L/2 \leq U \leq L$ depending on the zone corner bordering on the mass point. Likewise the integration must be carried out for the appropriate stresses along the line $U = L/2$ over the segment $0 \leq V \leq K/2$ or $K/2 \leq V \leq K$. Either the strain definitions (A8) and (A12) or (A9) and (A13) may be used. We will use the definitions (A8) and (A12) to correspond to the form in the text of the report. The integrations in either case are trivial

$$\begin{aligned}(F_{y'y'})_i^n &= \int_{x_1}^{x_2} [(2\mu + \lambda)\{(e + fU) \cos \theta - (b + cU) \sin \theta - 1\} \\ &\quad + \lambda\{(a + cK/2) \cos \theta + (d + fK/2) \sin \theta - 1\}]^n dU, \\ (F_{y'x'})_i^n &= \int_{x_1}^{x_2} [\mu\{(b + cU) \cos \theta + (e + fU) \sin \theta\}]^n dU,\end{aligned}\tag{A17}$$

where x_1 and x_2 are the appropriate limits either $x_1 = 0, x_2 = L/2$ or $x_1 = L/2, x_2 = L$, and

$$\begin{aligned}(F_{x'x'})_i^n &= \int_{x_3}^{x_4} [(2\mu + \lambda)\{(a + cV) \cos \phi - (d + fV) \sin \phi - 1\} \\ &\quad + \lambda\{(e + fL/2) \cos \phi + (b + cL/2) \sin \phi - 1\}]^n dV, \\ (F_{x'y'})_i^n &= \int_{x_3}^{x_4} [\mu\{(d + fV) \cos \phi + (a + cV) \sin \phi\}]^n dV,\end{aligned}\tag{A18}$$

where $x_3 = 0$, $x_4 = K/2$ or $x_3 = K/2$, $x_4 = K$ depending on the position of the zone about the mass point. Then

$$(F_{y'y'})_i^n = (2\mu + \lambda)_i^n [(e + \alpha fL/4) \cos \theta - (b + \alpha cL/4) \sin \theta - 1]_i^n L/2 \\ + \lambda_i^n [(a + cK/2) \cos \theta + (d + fK/2) \sin \theta - 1]_i^n L/2, \quad (\text{A19})$$

$$(F_{y'x'})_i^n = \mu_i^n [(b + \alpha cL/4) \cos \theta + (e + \alpha fL/4) \sin \theta]_i^n L/2,$$

and

$$(F_{x'x'})_i^n = (2\mu + \lambda)_i^n [(a + \alpha cK/4) \cos \phi - (d + \alpha fK/4) \sin \phi - 1]_i^n K/2 \\ + \lambda_i^n [(e + fL/2) \cos \phi + (b + cL/2) \sin \phi - 1]_i^n K/2, \quad (\text{A20})$$

$$(F_{x'y'})_i^n = \mu_i^n [(d + \alpha fK/4) \cos \phi + (a + \alpha cK/4) \sin \phi]_i^n K/2,$$

where the subscripts i denote the zone centers, for example those numbers enclosed in circles in Figure 3, in relation to mass point k , l , and n is the cycle number.

- $\alpha = 1$ for Equations (A19) for zones ① and ④,
- $\alpha = 1$ for Equations (A20) for zones ① and ②,
- $\alpha = 3$ for Equations (A19) for zones ② and ③,
- $\alpha = 3$ for Equations (A20) for zones ③ and ④.

As in the text, the first subscript designates the normal to the surface across which a stress in the direction of the second subscript is exerted. The primes on the subscripts denote that we are in a frame rotated with respect to the original frame.

We must then rotate these forces back to the original frame to apply them to the momentum equation.

$$(F_{y'x})_i^n = (F_{y'x'})_i^n \cos \theta^n - (F_{y'y'})_i^n \sin \theta^n, \quad (\text{A21})$$

$$(F_{y'y})_i^n = (F_{y'y'})_i^n \cos \theta^n + (F_{y'x'})_i^n \sin \theta^n,$$

and

$$(F_{x'x})_i^n = (F_{x'x'})_i^n \cos \phi^n + (F_{x'y'})_i^n \sin \phi^n, \quad (\text{A22})$$

$$(F_{x'y})_i^n = (F_{x'y'})_i^n \cos \phi^n - (F_{x'x'})_i^n \sin \phi^n.$$

The velocities can be computed from the force field by

$$\begin{aligned}\dot{x}_{k,l}^{n+1/2} &= \dot{x}_{k,l}^{n-1/2} + [(F_{x'x})_{\textcircled{1}} - (F_{x'x})_{\textcircled{2}} - (F_{x'x})_{\textcircled{3}} + (F_{x'x})_{\textcircled{4}} \\ &\quad + (F_{y'x})_{\textcircled{1}} + (F_{y'x})_{\textcircled{2}} - (F_{y'x})_{\textcircled{3}} - (F_{y'x})_{\textcircled{4}}]^n \Delta t^n / m_{k,l}, \\ \dot{y}_{k,l}^{n+1/2} &= \dot{y}_{k,l}^{n-1/2} + [(F_{y'y})_{\textcircled{1}} + (F_{y'y})_{\textcircled{2}} - (F_{y'y})_{\textcircled{3}} - (F_{y'y})_{\textcircled{4}} \\ &\quad + (F_{x'y})_{\textcircled{1}} - (F_{x'y})_{\textcircled{2}} - (F_{x'y})_{\textcircled{3}} + (F_{x'y})_{\textcircled{4}}]^n \Delta t^n / m_{k,l}.\end{aligned}\tag{A23}$$

The positions can be incremented by

$$\begin{aligned}x_{k,l}^{n+1} &= x_{k,l}^n + \dot{x}_{k,l}^{n+1/2} \Delta t^{n+1/2}, \\ y_{k,l}^{n+1} &= y_{k,l}^n + \dot{y}_{k,l}^{n+1/2} \Delta t^{n+1/2}.\end{aligned}\tag{A24}$$

E. TIME STEP

In accord with the Courant criterion, the time step is taken to be the minimum over the mesh of

$$\Delta t^{n+1/2} = C \Delta r^{n+1} / a,$$

where

$$\Delta r^{n+1} = A^{n+1} / S;$$

S is the longest diagonal of the quadrangle, a is the local dilatational wave speed and C has been taken to be 0.6.

F. GENERAL

The boundaries of the mesh can be treated as having phantom zones with no tractions, normal forces or masses. The code will not correctly calculate displacement disturbances with frequencies shorter than the time acquired for a dilatational disturbance to cross 4 zones. If these disturbances are produced on the boundaries of the mesh, dispersion of the induced wave trains is observed.

A tensor viscosity has been developed and used with the code.

REFERENCES

1. M. L. WILKINS, *Meth. Comp. Physics* **3**, 211 (1964).
2. T. H. H. PIAN, *Am. Inst. Aeron Astronaut J.* **2**, 576 (1964).
3. T. H. H. PIAN, *Am. Inst. Aeron Astronaut J.* **2**, 1333 (1964).

4. T. H. H. PIAN, in *Matrix Methods in Structural Mechanics* (Proceedings of the Conference held at Wright-Patterson Air Force Base, 26-28 October, 1965) Defense Documentation Center #AD 646300, p. 457.
5. S. TIMOSHENKO and D. H. YOUNG, "Advanced Dynamics," p. 311. McGraw-Hill, New York, 1948, or "Vibration Problems in Engineering," 3rd Ed., p. 351. D. van Nostrand, New York, 1955.
6. C. R. STEELE, *J. Appl. Mech.* **36**, 111 (1967). [Unfortunately, this author published four times the correct result].
7. J. M. WALSH, M. R. RILE, R. G. MCQUEEN, and F. L. YARGER, *Phys. Rev.* **108**, 196 (1957).